

STUDY OF SIZE-FRACTIONATED COAL-COMBUSTION AEROSOLS USING INSTRUMENTAL NEUTRON ACTIVATION ANALYSIS

W. MAENHAUT,* E. I. KAUPPINEN,** T. M. LIND**

**Institute for Nuclear Sciences, Proeftuinstraat 86, B-9000 Ghent (Belgium)*

***Technical Research Center of Finland (VTT), Laboratory of Heating and Ventilation (LVI), Tekniikkatie 4, SF-02150 (Finland)*

(Received September 22, 1992)

The chemical composition of aerosols emitted during coal combustion was studied as a function of particle size down to 0.01 μm . The aerosol collections were carried out in a 81 MW capacity boiler that burned Venezuelan coal in a circulating fluidized bed combustion chamber. The samples were collected upstream of the electrostatic precipitator using a Berner low-pressure impactor, which was equipped with a cyclone pre-cutter to avoid overloading of the first impaction stages. The samples were analyzed by INAA for up to about 40 elements. The elemental concentrations in the particulate matter for each impaction stage were plotted as a function of stage number (particle size). For the elements Na, Al, K, Ca, Sc, Ti, V, Ga, La and Sm, the concentration variation was limited to a factor of 2 to 4, and the concentrations of these elements were lower for the initial and final impactor stages than for the intermediate particle sizes. The variations were also limited to a factor of 2–4 for Mn, Fe, As, Sb and Th, but all these elements showed increasing concentrations with decreasing particle size. Still other elements, such as Ni, Cr, Co, Zn, W, Mo and the halogens, were highly enriched (up to 20–100 fold) in the fine particles when compared with the coarse particles.

Introduction

The chemical composition of particles emitted during coal combustion has been the subject of many studies since the early seventies. In several of these studies, the composition of aerosol particles formed in power plant scale combustion processes has been investigated as a function of particle size. Such measurements usually relied on bulk analysis of size-fractionated samples.¹⁻¹⁰ Occasionally, also techniques such as electron probe microanalysis (EPMA), which allow the analysis of individual particles, have been applied,¹¹⁻¹³ using then either size-segregated or total particulate samples. Especially the submicrometer particles, which are believed to be formed by nucleation of vaporized ash components and growth through coagulation and heterogeneous condensation, have received a lot of attention. Such particles are enriched in several potentially toxic constituents, have long residence times in the atmosphere and are able to penetrate into the alveoli of the lungs when inhaled.

The composition of fine combustion aerosols may vary considerably, though, depending upon the composition of the parent coal and on the combustion process. The great majority of studies have concentrated on pulverized coal boilers. Furthermore, few multielement data sets have been reported for size-fractionated particles

with diameters below about $0.3 \mu\text{m}$.⁷⁻¹⁰ Only KAUPPINEN and PAKKANEN¹⁰ have used a carefully calibrated low-pressure impactor to study real-scale pulverized coal-combustion aerosol characteristics below $0.3 \mu\text{m}$. In the present work, we studied the composition of particles from real-scale circulating fluidized bed coal combustion, and size fractions down to about $0.01 \mu\text{m}$ were examined. Results obtained so far, by using instrumental neutron activation analysis, are reported and briefly discussed.

Experimental

Sample collection

The samplings were carried out in an atmospheric pressure circulating fluidized bed, 81-MW fuel capacity coal boiler developed by Ahlstrom Corporation (Karhula, Finland). A schematic diagram of the boiler is shown in Fig. 1. A more detailed description of the circulating fluidized coal combustion system is given by TANG and TAYLOR.¹⁴ The samples were collected in-stack by drawing the flue gases isokinetically through a sampling train that consisted of a Berner low-pressure impactor

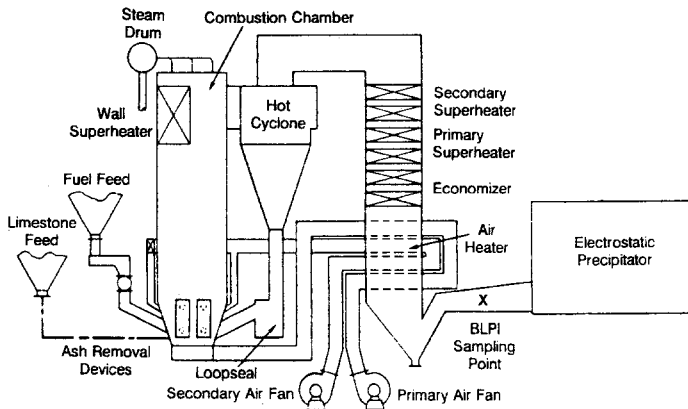


Fig. 1. Schematic diagram of the boiler

(BLPI, Hauke 25/0.015),^{15,16} preceded by a cyclone. As it was the aim to study the aerosol formation in the combustion process itself, samples were collected immediately before the entrance of the electrostatic precipitator at the flue gas temperature of about 120°C . The cyclone pre-cutter was added in order to avoid overloading of the upper BLPI stages, and collected approximately 90% of the particle mass. The estimated Stokes cut diameter (d_{50} value) of the pre-cutter was $5.4 \mu\text{m}$, so that the size distributions measured by the BLPI are only valid up to approximately that particle size. The BLPI is an 11-stage, multi-jet, compressible-flow low-pressure cascade impactor, with aerodynamic and Stokes cut diameters (d_{50} values) as given in Table 1. It is noteworthy that the aerodynamic cut diameters, as specified by the manufac-

turer,¹⁷ deviate significantly from those determined experimentally by HILLAMO and KAUPPINEN,¹⁸ particularly for stages 5 through 1. In this work, the Stokes cut diameters (last column of Table 1) are used. The collection substrates in the impactor consisted of annular polycarbonate films (poreless Nuclepore films), which were coated with a thin, homogeneous layer of Apiezon L vacuum grease according to a

Table 1
Aerodynamic and Stokes cut diameters (d_{50} values) for the Berner impactor (in μm)

Stage no.	D_p^*	D_p^{**}	D_p^+
11	16.	16.0	10.7
10	8.	7.62	5.5
9	4.0	3.77	2.6
8	2.0	1.90	1.4
7	1.0	0.949	0.64
6	0.5	0.517	0.30
5	0.25	0.326	0.17
4	0.125	0.163	0.07
3	0.060	0.0902	0.032
2	0.030	0.0617	0.021
1	0.015	0.0317	0.011

*Aerodynamic cut diameters specified by the manufacturer for a flow rate of 25 l/min and a temperature of 20 °C.¹⁷

**Aerodynamic cut diameters obtained by HILLAMO and KAUPPINEN for a flow rate of 24.6 l/min and a temperature of 20 °C.¹⁸

+Stokes cut diameters calculated according to HILLAMO and KAUPPINEN¹⁸ for a particle density of 2.45 g/cm³ and a temperature of 120 °C.

method described by HILLAMO and KAUPPINEN.¹⁸ The samples were collected in March and August 1990. The coal burned during the March experiment originated from Venezuela. It had an ash content of 4.1%, contained 37.5% volatiles and 58.4% fixed carbon (all expressed on a dry-sample basis). In the August experiment, the coal burned contained small amounts of English coal in addition to the coal from Venezuela. During the two experiments, a total of five real samples and three so-called in-situ blank samples were taken. For the latter, the flue gases were passed through two high-efficiency quartz fiber filters before entering the cyclone pre-cutter/BLPI sampling train. The purpose of these in-situ blank samples was to examine the effect of gaseous flue gas components on the measured particle composition. The sampling duration for both real samples and in-situ blanks was 20 or 30 s, and the volume of flue gas sampled was either 0.0065 or 0.0097 Nm³. All collection surfaces were weighed both before and after sampling, so that the particulate mass loading per stage could be determined.

Analysis

The impactor substrate films from stages 10 through 1 of all real samples and in-situ blanks were subjected to instrumental neutron activation analysis (INAA). One half of each annular film was used in the INAA, while the two remaining quarters

were reserved for analysis by particle-induced X-ray emission (PIXE) and inductively-coupled plasma mass spectrometry (ICP-MS). The INAA typically involved two separate irradiations of each sample (one of 5 minutes and one of 14 hours) at a flux of $1-3 \times 10^{12} \text{ n cm}^{-2} \text{ s}^{-1}$ in the Thetis reactor of the University of Ghent, and after each irradiation two or three gamma-spectrometric measurements with a high-resolution Ge detector were carried out. For two of the three in-situ blanks, however, the INAA was restricted to the short irradiation. The INAA procedures followed were similar to those described by MAENHAUT and ZOLLER¹⁹ and SCHUTYSER et al.,²⁰ and up to about 40 elements were measured. Besides the samples and in-situ blanks, unexposed greased blank polycarbonate films were also analyzed, and the blank values deduced from these films were used in deriving blank-corrected elemental masses for each of the ten impaction stages in each real sample and each in-situ blank. From these masses, the particulate masses deduced from weighing and the volume of flue gas sampled, particulate elemental concentrations in the flue gas (expressed in $\mu\text{g}/\text{Nm}^3$) and particle compositions were then derived.

Results and discussion

Concentrations in the flue gas, as obtained by summing over various impactor stages

For each element in each impactor sample, the concentrations in the flue gas were summed over stages 10 through 1, and over stages 7 through 1 (the submicrometer fraction), respectively. These summed concentrations were then averaged over the five real samples, on the one hand, and over the three in-situ blanks, on the other hand. The values, thus obtained, are listed in Table 2 for 29 elements and the particulate mass.

A comparison of the sums of the ten stages for the in-situ blanks with the similar data for the real samples indicates that the in-situ blank values amount to only a few percent of the real sample data for most elements. Clear exceptions are the halogens, particularly Cl and Br, where the in-situ blanks amount to 34% and 60% (the Br data for the in-situ blanks are semi-quantitative, though), and Cr and Ni, with in-situ blanks for both elements of about 28%. When we only consider the submicrometer size fraction (sum of stages 7 through 1), then the percentages found in the in-situ blanks (relative to the real samples) remain rather similar for the halogens, but for Cr and Ni, they have more than doubled, up to about 60%. The in-situ blank values also become quite appreciable for several other elements, particularly for Mn, Fe, Co, Zn and Mo (with submicrometer in-situ blank percentages varying between 20 and 40%). The occurrence of substantial amounts of halogens in the in-situ blanks is likely due to vapor phase condensation or adsorption of the gaseous halogen species on the greased impaction films or to reactions between these halogen species and the impaction films. The Cr and Ni in the in-situ blanks probably result from corrosion of the stainless-steel impactor by reactive gases.

The data in Table 2 also allow one to calculate what percentage of the various elements (and of the total particulate mass) occurs in the submicrometer size fraction (relative to the sum over the ten stages). Such calculation (for the real samples)

Table 2
Average concentrations in the real samples and the in-situ blanks for 29 elements and the particulate mass (MS). Data are in $\mu\text{g}/\text{Nm}^3$ for the elements, and in mg/Nm^3 for MS

Element	Sum over stages 10 through 1		Sum over stages 7 through 1	
	real samples $\bar{x} \pm s$ (N)*	in-situ blanks $\bar{x} \pm s$ (N)	real samples $\bar{x} \pm s$ (N)	in-situ blanks $\bar{x} \pm s$ (N)
Na	4100 \pm 1200(5)	47 \pm 14(3)	580 \pm 270(5)	15.2 (1)
Mg	16800 \pm 2300(5)	330 \pm 220(3)	1630 \pm 450(5)	266 (1)
Al	92000 \pm 17000(5)	1010 \pm 270(3)	10600 \pm 4800(5)	240 \pm 130(3)
Cl	7600 \pm 6500(5)	2610 \pm 1310(3)	4400 \pm 4200(5)	1440 \pm 620(3)
K	8400 \pm 1700(5)	122 (1)	1270 \pm 500(5)	56 (1)
Ca	147000 \pm 10000(5)	2300 \pm 1600(3)	13400 \pm 1700(5)	620 \pm 770(3)
Sc	17.2 \pm 1.9(5)	0.156 (1)	3.6 \pm 0.8(5)	0.020 (1)
Ti	5300 \pm 500(5)	64 \pm 33(3)	930 \pm 340(5)	20.3 \pm 13.1(3)
V	155 \pm 15(5)	3.5 \pm 1.5(3)	28.9 \pm 8.3(5)	1.63 \pm 1.02(3)
Cr	660 \pm 390(5)	183 (1)	300 \pm 140(5)	183 (1)
Mn	460 \pm 90(5)	46 \pm 33(3)	74 \pm 46(5)	28.7 \pm 17.1(3)
Fe	26500 \pm 6900(5)	1510 (1)	4200 \pm 2200(5)	950 (1)
Co	24.5 \pm 5.6(5)	1.79 (1)	5.7 \pm 2.3(5)	1.54 (1)
Ni	420 \pm 220(5)	116 (1)	177 \pm 76(5)	109 (1)
Zn	163 \pm 18(5)	13.9 (1)	37 \pm 12(5)	13.9 (1)
Ga	20.8 \pm 3.7(5)	0.140 (1)	4.2 \pm 1.4(5)	
As	7.7 \pm 1.7(5)	0.22 (1)	1.10 \pm 0.20(5)	0.077 (1)
Se	180 \pm 31(5)	1.41 (1)	37 \pm 10(5)	
Br	46 \pm 26(5)	28 (3)	22.0 \pm 17.0(5)	17 (3)
Sr	650 \pm 150(5)		103 \pm 62(5)	
Mo	31 \pm 9(5)	3.9 (1)	11.4 \pm 5.7(5)	3.9 (1)
Sb	3.1 \pm 0.1(5)	0.132 (1)	0.58 \pm 0.09(5)	0.050 (1)
I	35 \pm 5(5)	4.7 \pm 2.7(3)	11.1 \pm 3.8(5)	2.22 \pm 1.50(3)
Ba	540 \pm 67(5)	9.3 \pm 2.5(2)	88 \pm 49(5)	
La	33 \pm 6(5)	0.42 (1)	5.7 \pm 2.2(5)	0.125 (1)
Sm	6.2 \pm 0.9(5)	0.064 (1)	1.04 \pm 0.36(5)	0.0144 (1)
Eu	1.69 \pm 0.40(5)	0.149 (1)	0.55 \pm 0.26(5)	0.078 (1)
W	6.9 \pm 4.3(5)	0.70 (1)	3.8 \pm 2.5(5)	0.55 (1)
Th	11.4 \pm 1.8(5)		1.95 \pm 0.68(5)	
MS	1200 \pm 140(5)	69 \pm 13(3)	146 \pm 32(5)	28.6 \pm 6.0(3)

*Data are averages and standard deviations, based on N samples.

reveals fine fraction percentages that are typically between 10 and 20%. Exceptions are the halogens, Cr and Ni, and Mo, Eu and W, which all exhibit fine percentages between 30 and 60%.

Average mass size distributions

Mass size distributions (with the percentage of mass per stage as a function of stage number) were calculated for each element in each individual impactor sample, and subsequently averaged over, on the one hand, the five real samples, and, on the other hand, the three in-situ blanks. Fig. 2 presents the average mass size distributions for nine elements and the particulate mass in the real samples. On the left side of the figure are elements that are predominantly associated with the coarse particles,

whereas the right side displays elements that exhibit a flatter size distribution. The shape of the size distribution is affected by the pre-cutter cyclone above approximately 3 μm , because the cyclone collection efficiency curve is not a step function at the cut-point particle size, but a rather slowly rising S-shaped curve.

In several of the size distributions of Fig. 2 (i.e., those for the particulate mass, Br, I, Mo and to a lesser extent for As and Zn) one can discern a distinct very fine

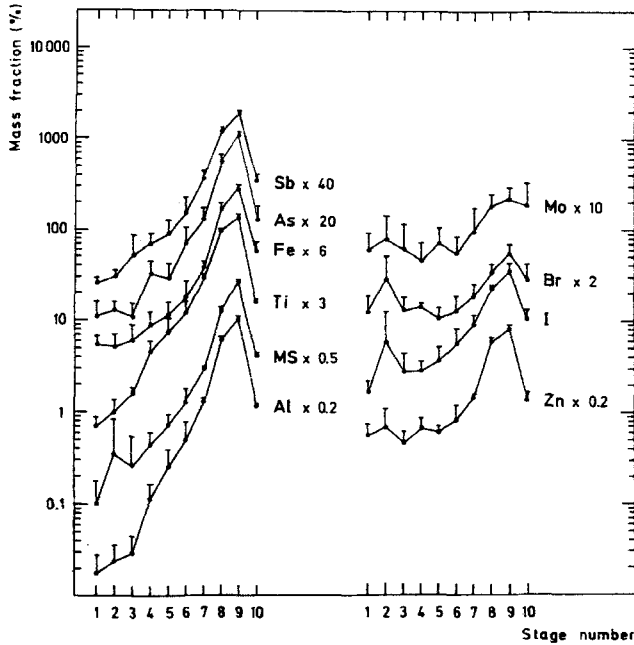


Fig. 2. Average size distributions for nine elements and the particulate mass (MS) in the real samples. The half error bar indicates the standard deviation, as calculated from the spread in the data for the five samples

mode, with its center at stage 2 (that is, with a particle diameter of 0.02–0.03 μm). Of the elements not shown in Fig. 2, Cl and W also exhibited this very fine mode. The existence of such fine mode in the aerosol emissions from coal-fired boilers was first identified by McELROY et al.,⁷ who studied aerosols upstream of the particulate control device in pulverized coal boilers. The fine mode contained 0.2 to 2.2% of the total fly ash mass in that study, but in other studies of aerosols upstream of the particulate control device higher particulate mass percentages in the fine mode have been observed.⁹ As the BLPI collected only about 10% of the total particulate mass, the ash mass fraction in the fine mode observed here is significantly below the range given by McELROY et al.⁷ Additional differences between our results and previous studies seem to reside in the position of the peak in that fine mode and in the number of elements exhibiting this mode. Normally, this peak occurs between 0.04

and 0.15 μm in diameter, thus at higher particle diameter than here, and many more elements (often including even lithophilic elements) show that fine mode.^{7,9,10}

Another important observation that can be made from Fig. 2 is that the size distributions of the various elements deviate from each other and from that of the particulate mass. This implies that the composition of the particles is clearly size-dependent.

The average size distributions obtained for the in-situ blanks (not shown here) tended to be much flatter than those for the real samples, except for the halogens.

Particulate composition as a function of particle size

For each of the stages 10 through 5 in each of the five real samples, the elemental concentrations in the collected particulates were calculated (in $\mu\text{g/g}$), and averages (for each stage over the five samples) and associated standard deviations were subsequently derived. Because of the low collected particle masses relative to the tare weights of the impaction films for stages 4 through 1, the precision of the particle mass measurement was quite poor for these stages (many elements measured by INAA do not suffer from this). Therefore, for each of these stages, the ratios of the elemental mass to the Al mass were calculated and then averaged over all five samples, and these averages were multiplied by the average Al concentration in the particulate mass, whereby the latter had been calculated with evident outliers removed (i.e., the Al concentration in the particulate mass for stages 3 and 1 of one sample was rejected). Furthermore, the standard deviation of the average Al concentration in the particulate mass was not retained in the error propagating calculations, so that the standard deviation associated with the concentration of an element X for stages 4 through 1 reflects in fact only the variability in the X/Al mass ratios.

In investigations of the composition of coal-combustion aerosols, it is quite common to make a comparison with the composition of average crustal rock, and a good resemblance between the two compositions is often noted. Therefore, the average elemental concentrations in the collected particles, calculated as described above, were normalized by the concentrations in MASON's average crustal rock.²¹ The normalized concentrations, thus defined, are quite similar to the often-used crustal enrichment factors (EFs), the difference being that only a single normalization is carried out here, versus a double normalization, using a reference element (typically Al or Fe), in EF calculations.

Plots of the normalized average concentration in the particulate matter as a function of particle size were made for 29 elements, and are shown in Figs 3-7. Fig. 3 groups the elements Na, Al, K, Ca, Sc, Ti, V, Ga, La and Sm. Several of these elements occur in the mineral fraction of coal and are lithophilic elements. The normalized concentration for all ten elements varies rather little as a function of particle size (the variation remains limited to a factor of 2 to 4), and, interestingly, the concentrations are lower for the initial and final impactor stages than for the intermediate particle sizes. Furthermore, the normalized concentrations are generally close to 1, except for Na and K, which are depleted in the fly ash relative to crustal rock. Both elements are likely also depleted in the input coal. The behavior for the elements plotted in Fig. 3 is generally consistent with that observed in previous investigations. In their study on pulverized coal-combustion aerosols (where the particles were col-

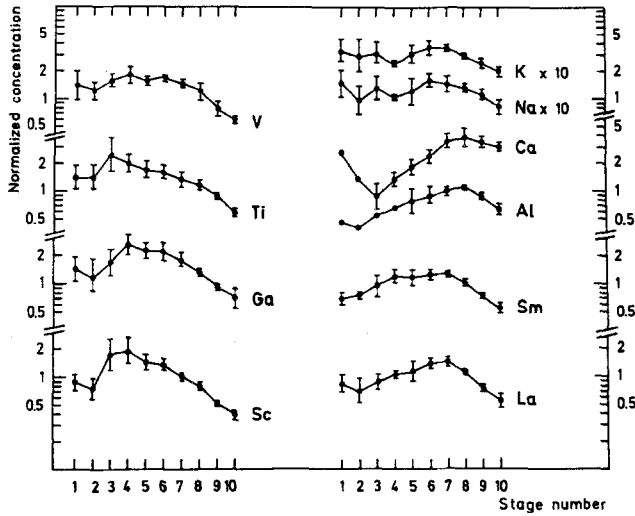


Fig. 3. Average normalized concentrations for ten elements in the five real samples. The error bar indicates the standard deviation, as calculated from the spread in the data for the five samples

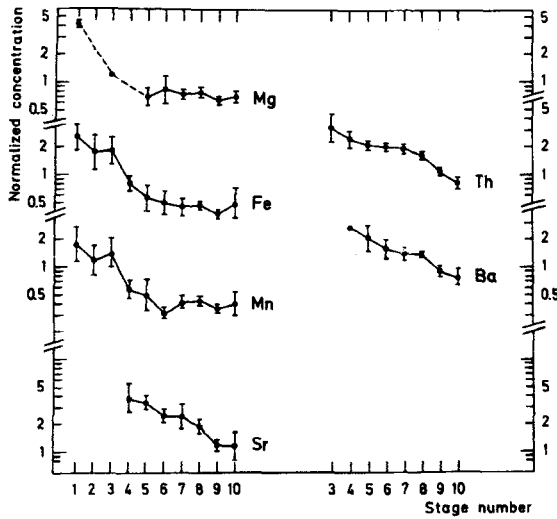


Fig. 4. Average normalized concentrations for six elements in the five real samples. The error bar indicates the standard deviation, as calculated from the spread in the data for the five samples

lected with a BLPI after the electrostatic precipitator), KAUPPINEN and PAKKANEN¹⁰ observed shapes similar to those in Fig. 3 for the elements Na, Mg, Al, Si, K, Ti, Fe and Mn. For Ca and particularly V, however, the concentration increased steeply with decreasing particle size in that study. Slight V and Ca enrichments in the

fine particles were also observed by MARKOWSKI and FILBY.⁹ The latter authors also observed that the Ga concentration increased steeply with decreasing particle size, which is in contrast with what is found here.

For the elements shown in Figs 4-7, with the exception of Se, the normalized concentration increases with decreasing particle size, but there is a large difference in the

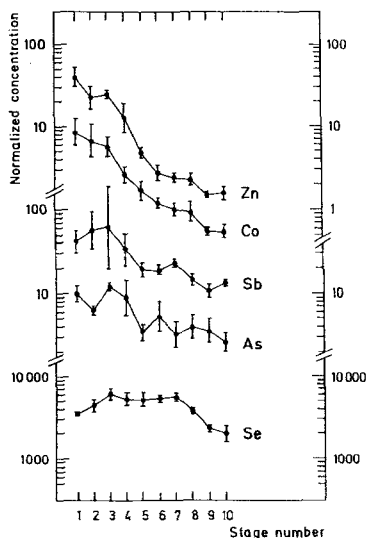


Fig. 5. Average normalized concentrations for five elements in the five real samples. The error bar indicates the standard deviation, as calculated from the spread in the data for the five samples

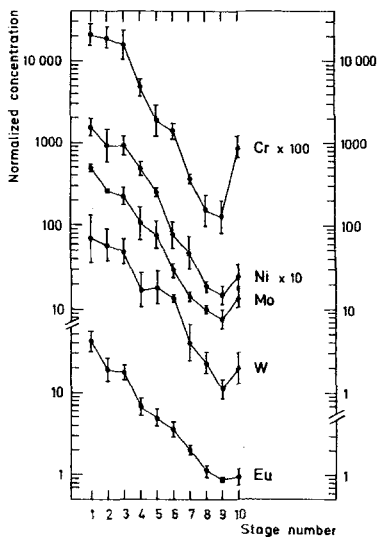


Fig. 6. Average normalized concentrations for five elements in the five real samples. The error bar indicates the standard deviation, as calculated from the spread in the data for the five samples

slope of that increase. For Mg, Mn, Fe, Sr, Ba and Th (grouped in Fig. 4), and also for As and Sb (Fig. 5), the increase remains limited to a factor of 2 to 4. Usually, As and Sb exhibit much larger fine-particle enrichments than those seen here. For example, MARKOWSKI and FILBY⁹ observed that the As/Fe and the Sb/Fe ratios in particles less than $0.1 \mu\text{m}$ were respectively 20 and 40 times higher than the corresponding ratios in particles of $1\text{--}10 \mu\text{m}$ diameter.

The element Se (Fig. 5) shows somewhat peculiar behavior. The shape of the normalized concentration plot shows close resemblance to that of the elements grouped in Fig. 3, with lower concentrations in the fine and coarse particles than in the intermediate-sized particles. Selenium is usually highly enriched in the fine-particle fraction when compared with the coarse particles (e.g., ONDOV et al.,⁶ MARKOWSKI and FILBY⁹). However, rather constant concentrations (or Se/Fe ratios) as a function of particle size have also been observed.⁷ The normalized Se concentrations in Fig. 5 vary from about 2000 to 6000, indicating that Se is highly enriched with respect to

crustal rock. However, this large enrichment is most likely mainly due to the fact that Se is also highly enriched in the input coal.

The elements Co and Zn (Fig. 5), Cr, Ni, Mo, Eu and W (Fig. 6), and the halogens (Fig. 7) all show a very steeply increasing concentration with decreasing particle size. In fact, these elements are typically between 20 and 100 times more concentrated in the very fine particles than in the coarse ones. Such high fine-particle

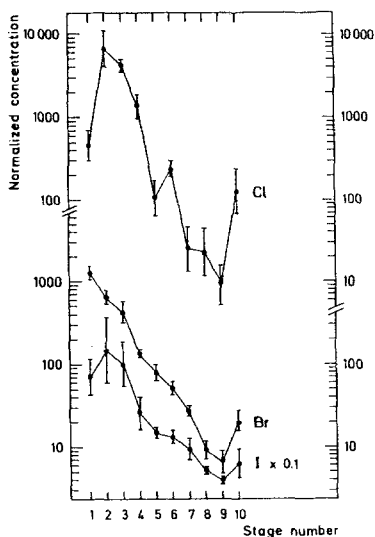


Fig. 7. Average normalized concentrations for three halogens in the five real samples. The error bar indicates the standard deviation, as calculated from the spread in the data for the five samples

enrichments have rarely been observed in previous studies, but, then, only a few of these elements have been reported in detailed studies on the composition of size-fractionated coal-combustion aerosols. McELROY et al.⁷ observed that the Zn/Fe ratio was about 10 times higher in particles less than 0.3 μm than in particles of 10 μm diameter. A high fine-particle enrichment for W (of about a factor of 40) was noted by ONDOV et al.⁶ For several of the elements shown in Figs. 6 and 7, our data should be considered with caution, though. As discussed above, our Cr and Ni data are likely affected by contamination. Also, for the halogens, particularly Cl and Br, our data do not really represent the actual aerosol particle composition in the stack, but are influenced by artifacts that take place during sampling.

*

W. M. is grateful to the Belgian "Nationaal Fonds voor Wetenschappelijk Onderzoek" and the "Interuniversitair Instituut voor Kernwetenschappen" for financial support. E. I. K. and T. M. L. gratefully acknowledge financial support through the Finnish combustion research program LIEKKI. The authors thank R. KUIVALAINEN and H. VILOKKI from H. Ahlstrom Laboratories, A. MEHTONEN from VTT/LVI and the plant operation personnel for their help during the field experiments. Thanks are also due to V. BAEKE, C. GILOT and J. CAFMEYER for their assistance in the neutron activation analysis.

References

1. R. L. DAVISON, D. F. S. NATUSCH, J. R. WALLACE, C. A. EVANS, Jr., *Environ. Sci. Technol.*, 13 (1974) 1107.
2. C. BLOCK, R. DAMS, *Environ. Sci. Technol.*, 10 (1976) 1011.
3. E. S. GLADNEY, J. A. SMALL, G. E. GORDON, W. H. ZOLLER, *Atmos. Environ.*, 10 (1976) 1071.
4. R. D. SMITH, J. A. CAMPBELL, K. K. NIELSON, *Environ. Sci. Technol.*, 13 (1979) 553.
5. J. M. ONDOV, R. C. RAGAINI, A. H. BIERMANN, *Environ. Sci. Technol.*, 13 (1979) 598.
6. J. M. ONDOV, R. C. RAGAINI, A. H. BIERMANN, *Environ. Sci. Technol.*, 13 (1979) 946.
7. M. W. McELROY, R. C. CARR, D. S. ENSOR, G. R. MARKOWSKI, *Science*, 215 (1982) 13.
8. A. D. SHENDRIKAR, D. S. ENSOR, S. J. COWEN, G. J. WOFFINDEN, M. W. McELROY, *Atmos. Environ.*, 17 (1983) 1411.
9. G. R. MARKOWSKI, R. FILBY, *Environ. Sci. Technol.*, 19 (1985) 796.
10. E. I. KAUPPINEN, T. A. PAKKANEN, *Environ. Sci. Technol.*, 24 (1990) 1811.
11. R. D. SMITH, J. A. CAMPBELL, K. K. NIELSON, *Atmos. Environ.*, 13 (1979) 607.
12. N. KAUFHERR, D. LICHTMAN, *Environ. Sci. Technol.*, 18 (1984) 544.
13. Y. MAMAME, J. L. MILLER, T. G. DZUBAY, *Atmos. Environ.*, 20 (1986) 2125.
14. J. T. TANG, E. S. TAYLOR, in: *Atmospheric Fluidized Bed Combustion, A Technical Source Book*, S.-E. TUNG, G. C. WILLIAMS (Eds), USDOE/MC/14536-2544, Jan. 1987, p. 188.
15. A. BERNER, *Staub-Reinhalt. Luft*, 32 (1972) 315.
16. A. BERNER, C. LURZER, *J. Phys. Chem.*, 84 (1980) 2079.
17. HAUKE KG, *Instruction Manual for Hauke Low Pressure Impactor*, 1984.
18. R. E. HILLAMO, E. I. KAUPPINEN, *Aerosol Sci. Technol.*, 14 (1991) 33.
19. W. MAENHAUT, W. H. ZOLLER, *J. Radioanal. Chem.*, 37 (1977) 637.
20. P. SCHUTYSER, W. MAENHAUT, R. DAMS, *Anal. Chim. Acta*, 100 (1978) 75.
21. B. MASON, *Principles of Geochemistry*, 3rd ed., John Wiley, New York, 1966.